

Randomness and Emerging Order in Nuclear Structure

R. Bijker¹ and A. Frank^{1,2}

¹Instituto de Ciencias Nucleares, Universidad Nacional Autónoma de México,
Apartado Postal 70-543, 04510 México, D.F., México

²Centro de Ciencias Físicas, Universidad Nacional Autónoma de México,
Apartado Postal 139-B, Cuernavaca, Morelos, México

November 23, 2018

Abstract

In order to investigate to what extent is the low-lying behavior of even-even nuclei dependent on particular nucleon-nucleon interactions, we consider systems of bosons where these interactions are taken as gaussian random numbers with equal likelihood of being attractive or repulsive. We find a statistical dominance of $L = 0$ ground states and other correlations, which we analyze in terms of a mean field approach.

Para investigar hasta que punto el comportamiento de los núcleos está determinado por interacciones particulares entre los nucleones, consideramos sistemas de bosones con interacciones gaussianas aleatorias, donde dichas interacciones tienen la misma probabilidad de ser atractivas o repulsivas. Encontramos un dominio estadístico de estados base $L = 0$ y otras correlaciones, que analizamos en términos de un método de campo medio.

PACS numbers: 05.30.Jp, 21.60.Ev, 21.60.Fw, 24.60.Lz

1 Introduction

Whereas conventional wisdom ascribes the observed properties of low-lying nuclear systems to a particular form of the nucleon-nucleon interaction, recent investigations have found that some of these features may represent a general and robust property of many-body systems [1]-[7]. Random matrices have been used in the past in order to study generic spectral properties, but the emphasis was usually centered on global characteristics, such as level-spacing distributions in highly excited nuclei or the average properties of small metallic particles or quantum dots [8]. This approach had its origin in the observation by E.P. Wigner that ‘... *the Hamiltonian which governs the behavior of a complicated system is a random symmetric matrix, with no particular properties except for its symmetric nature*’. At high energy, nuclear dynamics is thus assumed to have lost track of any correlations. In the case of other systems, random fluctuations in shapes and/or impurities can be reasonably modeled in this form and their average properties reproduced.

A general conclusion of these studies is that the specific mechanism (interactions) seem to be irrelevant in the determination of global features.

However, the random-matrix analyses of nuclear distributions typically involve states with the same quantum numbers, such as angular momentum, parity or isospin, and little attention was given to correlations among different symmetries. Although the so-called two-body random ensemble (TBRE) was

defined long time ago and some of its properties investigated [9, 10], again attention was focused mostly on its global features and not so much on low-lying patterns [8]. This kind of ensemble is associated with a random selection of the two-body matrix elements, while the n -body Hamiltonian matrices are generated with the usual coupling procedures. On the other hand, it is known that nuclei display very regular spectral properties. For example, in Refs. [11, 12] an analysis of energy systematics of medium and heavy even-even nuclei suggests a classification in terms of seniority, anharmonic vibrator and rotor regions. Plots of the excitation energies of the yrast states with $L^P = 4^+$ against $L^P = 2^+$ show characteristic slopes for each region. This and other correlations have been shown to be robust features of low-energy nuclear behavior which signal the emergence of order and collectivity. In each case this behavior has been shown to arise from particular nucleon-nucleon interactions, such as an attractive pairing force in semimagic nuclei and the strongly attractive neutron-proton quadrupole-quadrupole interaction for deformed nuclei. It came as a surprise, therefore, that recent studies for even-even nuclei, in a shell model with randomly distributed two-body interactions (TBRE), displayed a marked statistical preference for $L^P = 0^+$ ground states, energy gaps, and other indicators of ordered behavior [1]. These results sparked a large number of other numerical and theoretical investigations, in both fermion [2, 3, 6, 7, 13, 14] and boson systems [4, 5, 7, 15, 16, 17], in an attempt to explain this remarkable and unexpected results.

In this contribution we summarize some of the most notable findings in the context of the Interacting Boson Model (IBM) and present a possible explanation in terms of a mean-field analysis. In the conclusions we indicate some of the many remaining open questions and future research.

2 The interacting boson model

The IBM describes low-lying collective excitations in nuclei in terms of a system of N interacting monopole and quadrupole bosons [18]. An analysis of the IBM with random one- and two-body interactions gave rise to further statistical evidence of spontaneous emergence of order, manifested by a large percentage of ground states with $L^P = 0^+$ and clear vibrational and rotational correlations [4, 5]. Fig. 1 shows that there is a predominance (63.4 %) of $L^P = 0^+$ ground states; in 13.8 % of the cases the ground state has $L^P = 2^+$, and in 16.7 % it has the maximum value of the angular momentum $L^P = 32^+$. For the cases with a $L^P = 0^+$ ground state, we show in Fig. 2 the probability distribution of the energy ratio

$$R = \frac{E_{4_1^+} - E_{0_1^+}}{E_{2_1^+} - E_{0_1^+}}. \quad (1)$$

There are two very pronounced peaks, right at the vibrational value of $R = 2$ and at the rotational value of $R = 10/3$, a clear indication of the occurrence of vibrational and rotational structure. This is confirmed by a simultaneous study of the quadrupole transitions between the levels [4].

These are surprising results in the sense that, according to the conventional ideas in the field, the occurrence of $L = 0$ ground states and the existence of vibrational and rotational bands are due to very specific forms of the interactions. The study of the IBM Hamiltonian with random one- and two-body interactions seems to indicate that this may not be the entire story. However, the above results were obtained from numerical studies. It would be very interesting to gain a better understanding as to why this happens. What is the origin of the regular features which arise from random (both in sign and size) interactions? In this respect, there is a relevant quote by E.P. Wigner (as communicated to us by M. Moshinsky): *‘I am happy to learn that the computer understands the problem, but I would like to understand it too’.*

In the next sections, we report on an attempt in this direction by considering the vibron model, which has the same qualitative features as the IBM, namely vibrational and rotational spectra, but has a much simpler mathematical structure, since there are no coefficients of fractional parentage (cfp’s). All many-body matrix elements can be derived in closed analytic form [19, 20].

3 The vibron model

The vibron model is an interacting boson model designed to describe the relative motion in two-body problems, e.g. diatomic molecules [21], nuclear clusters [22] and mesons [23]. Its building blocks are a dipole boson p^\dagger with $L^P = 1^-$ and a scalar boson s^\dagger with $L^P = 0^+$. The total number of bosons N is conserved by the vibron Hamiltonian. Here we only consider to one- and two-body interactions

$$H = \frac{1}{N} \left[H_1 + \frac{1}{N-1} H_2 \right], \quad (2)$$

where H_1 contains the boson energies

$$H_1 = \epsilon_s s^\dagger \cdot \tilde{s} - \epsilon_p p^\dagger \cdot \tilde{p}, \quad (3)$$

and H_2 all possible two-body interactions

$$\begin{aligned} H_2 = & u_0 \frac{1}{2} (s^\dagger \times s^\dagger)^{(0)} \cdot (\tilde{s} \times \tilde{s})^{(0)} + u_1 (s^\dagger \times p^\dagger)^{(1)} \cdot (\tilde{p} \times \tilde{s})^{(1)} \\ & + \sum_{\lambda=0,2} c_\lambda \frac{1}{2} (p^\dagger \times p^\dagger)^{(\lambda)} \cdot (\tilde{p} \times \tilde{p})^{(\lambda)} \\ & + v_0 \frac{1}{2\sqrt{2}} \left[(p^\dagger \times p^\dagger)^{(0)} \cdot (\tilde{s} \times \tilde{s})^{(0)} + H.c. \right], \end{aligned} \quad (4)$$

and $\tilde{p}_m = (-1)^{1-m} p_{-m}$. We have scaled H_1 by N and H_2 by $N(N-1)$ in order to remove the N dependence of the matrix elements.

We first carry out a numerical study of the vibron model using random one- and two-body interactions. The seven parameters of the Hamiltonian altogether denoted by

$$(\vec{x}) \equiv (\epsilon_s, \epsilon_p, u_0, u_1, c_0, c_2, v_0), \quad (5)$$

are taken as independent random numbers on a Gaussian distribution

$$P(x_i) = e^{-x_i^2/2\sigma^2} / \sigma\sqrt{2\pi}, \quad (6)$$

with zero mean and width σ . In Fig. 3 we show the percentages of $L = 0$, $L = 1$ and $L = N$ ground states as a function of the total number of vibrons N . Just as for the IBM, the vibron model shows a dominance of $L = 0$ ground states. For even values of N the ground state has $L = 0$ in ~ 71 % of the cases, and for odd values in ~ 55 % of the cases. Similarly, the percentage of ground states with $L = 1$ shows an oscillation between ~ 1 % for even values of N and ~ 18 % for odd values. In ~ 24 % of the cases the ground state has the maximum value of the angular momentum $L = N$.

For the cases with a $L^P = 0^+$ ground state, we show in Figs. 4 and 5 the probability distribution of the energy ratio

$$R = \frac{E_{2_1^+} - E_{0_1^+}}{E_{1_1^-} - E_{0_1^+}}. \quad (7)$$

In the vibrational limit the spectrum is that of a three-dimensional harmonic oscillator with $R = 2$, and in the rotational limit that of a three-dimensional Morse oscillator with $R = 3$. Both for even and odd values of N we see two clear peaks, one at the vibrational value of $R = 2$ and one at the rotational value of $R = 3$. Moreover, for even values of N there is a peak at $R = 0$, which is absent for odd values, as we shall prove below.

This numerical study confirms that the vibron model exhibits the same regular features as does the IBM, although there are some differences as well. Now the question is, how can we understand these properties in an analytic and more intuitive way? In a recent study the tridiagonal form of the Hamiltonian matrix of the vibron model was used to establish a connection with random polynomials [16, 17]. However, in general the Hamiltonian matrix is not of this form, and one has to look for alternative methods.

In the next section we show that a mean-field study of the vibron model with random interactions can account for all features that were discussed above.

4 Mean-field analysis

The connection between the vibron model, potential energy surfaces, equilibrium configurations, shapes, etc., can be studied by means of coherent states. The coherent state for the vibron model can be written as a condensate of a deformed boson which is a superposition of a scalar and a dipole boson [24]

$$|N, \alpha\rangle = \frac{1}{\sqrt{N!}} \left(\sqrt{1 - \alpha^2} s^\dagger + \alpha p_0^\dagger \right)^N |0\rangle, \quad (8)$$

with $0 \leq \alpha \leq 1$. The potential energy surface is then given by the expectation value of the Hamiltonian in the coherent state

$$E_N(\alpha) = \langle N, \alpha | H | N, \alpha \rangle = a_4 \alpha^4 + a_2 \alpha^2 + a_0, \quad (9)$$

where the coefficients a_i are linear combinations of the parameters of the Hamiltonian

$$\begin{aligned} a_4 &= \vec{r} \cdot \vec{x} = \frac{1}{2}u_0 + u_1 + \frac{1}{6}c_0 + \frac{1}{3}c_2 + \frac{1}{\sqrt{6}}v_0, \\ a_2 &= \vec{s} \cdot \vec{x} = -\epsilon_s + \epsilon_p - u_0 - u_1 - \frac{1}{\sqrt{6}}v_0, \\ a_0 &= \epsilon_s + \frac{1}{2}u_0. \end{aligned} \quad (10)$$

For random interactions, we expect the trial wave function of Eq. (8) and the energy surface of Eq. (9) to provide information on the distribution of shapes that the model can acquire. The equilibrium configuration is characterized by the value of $\alpha = \alpha_0$ for which the energy surface $E_N(\alpha)$ has its minimum value. For a given Hamiltonian, the value of α_0 depends on the coefficients a_4 and a_2 . The distribution of shapes for an ensemble of Hamiltonians depends on the joint probability distribution of the coefficients a_4 and a_2

$$\begin{aligned} P(a_4, a_2) &= \int \prod_i dx_i P(x_i) \delta(a_4 - \vec{r} \cdot \vec{x}) \delta(a_2 - \vec{s} \cdot \vec{x}) \\ &= \frac{1}{2\pi \det M} \exp \left[-\frac{1}{2} \begin{pmatrix} a_4 & a_2 \end{pmatrix} M^{-1} \begin{pmatrix} a_4 \\ a_2 \end{pmatrix} \right], \end{aligned} \quad (11)$$

where $P(x_i)$ is given by Eq.(6) and

$$M = \begin{pmatrix} \vec{r} \cdot \vec{r} & \vec{r} \cdot \vec{s} \\ \vec{r} \cdot \vec{s} & \vec{s} \cdot \vec{s} \end{pmatrix}. \quad (12)$$

The vectors \vec{r} and \vec{s} are defined in Eq. (10). In this approximation, we find that there are only three possible equilibrium configurations:

- $\alpha_0 = 0$: s -boson condensate. This corresponds to a spherical shape whose probability can be obtained by integrating $P(a_4, a_2)$ over the appropriate range S_1

$$\begin{aligned} P_1 &= \int_{S_1} da_4 da_2 P(a_4, a_2) \\ &= \frac{1}{4\pi} \left[\pi + 2 \arctan \left(\frac{|\vec{s} \cdot \vec{s} + \vec{r} \cdot \vec{s}|}{\sqrt{\det M}} \right) \right] = 0.396 . \end{aligned} \quad (13)$$

This configuration has spherical symmetry and hence can only have $L = 0$.

- $0 < \alpha_0 < 1$: deformed condensate. The probability for the occurrence of a deformed shape can be calculated in a similar way and is given by

$$P_2 = \frac{1}{2\pi} \arctan \left(\frac{2\sqrt{\det M}}{\vec{s} \cdot \vec{s} + 2\vec{r} \cdot \vec{s}} \right) = 0.216 . \quad (14)$$

A deformed shape corresponds to a rotational band with angular momenta $L = 0, 1, \dots, N$.

- $\alpha_0 = 1$. The probability for finding the third solution, a p -boson condensate, is given by

$$P_3 = 1 - P_1 - P_2 = 0.388 .$$

The angular momentum content of a p -boson condensate is $L = N, N - 2, \dots, 1$ for N odd or $L = N, N - 2, \dots, 0$ for N even.

The probability that the ground state has $L = 0$ can be estimated by assuming a complete decoupling of vibrations and rotations. For N even this gives $\frac{1}{2}(1 + P_1)$ or 69.8 %, and for N odd we have $P_1 + \frac{1}{2}P_2$ or 50.4 %, in good agreement with the numerical values. In Table 1 we show the probabilities and corresponding percentages for the ground states with angular momentum $L = 0, 1$ and N .

A better estimate can be obtained by evaluating the moment of inertia. We adopt the Thouless-Valatin prescription, which leads to the formula

$$\mathcal{I} = \frac{2N\alpha_0^2}{4(N-1) \left[\frac{1}{2\sqrt{6}}v_0(1 - \alpha_0^2) - \frac{1}{6}(c_0 - c_2)\alpha_0^2 \right]} . \quad (15)$$

The moment of inertia thus depends in a complicated way on the parameters in the Hamiltonian, both explicitly as seen in the denominator of Eq. (15) and implicitly through α_0 , which determines the equilibrium configuration. Formally, the probability to find a $L = 0$ ground state is determined by the integral of the joint probability distribution $P(a_4, a_2, \mathcal{I})$ over the appropriate range. The results are summarized in Table 2. The spherical shape corresponds to an energy ratio of $R = 2$, and the deformed shape to $R = 3$. This explains the vibrational and rotational peaks observed in Fig. 4 and 5. The occurrence of a peak at $R = 0$ for even values of N is related to the p -boson condensate solution, which has angular momenta $L = 0, 2, \dots, N$. The first excited $L = 1$ state belongs to a different band and has a higher excitation energy. For odd values of N the p -boson condensate has no state with $L = 0$, and hence the peak at $R = 0$ is absent.

In Fig. 6 we show the percentages of $L = 0$, $L = 1$ and $L = N$ ground states, as calculated in the mean-field analysis. A comparison with the exact results of Fig. 3 shows that the mean-field results are in excellent agreement with the exact ones. The oscillations in the percentages of $L = 0$ and $L = 1$ ground states are entirely due to the angular momentum decomposition of the p -boson condensate, whereas the percentage of ground states with the maximum value of the angular momentum $L = N$ is a constant and does not depend on N .

5 Summary and conclusions

In this contribution, we have studied the properties of low-lying collective levels in the interacting boson model and the vibron model with random interactions. In particular, we discussed the dominance of $L = 0$ ground states and the occurrence of vibrational and rotational band structures. In both models these features represent general and robust properties, and are a consequence of the many-body dynamics.

We have studied the origin of these regular features in more detail in the context of the vibron model. In a mean-field analysis of the vibron model with random interactions it was found that we can account for all observed features, both qualitatively and quantitatively. The occurrence of $L = 0$ ground states can be related to the different equilibrium configurations of the vibron model. There are three different equilibrium configurations: a spherical shape (40 %), a deformed shape (20 %) and a condensate of dipole bosons (40 %). Since the spherical shape only has $L = 0$, and the deformed shape and the p -boson condensate with N even in about half the number of cases, one finds a $L = 0$ ground state in approximately 70 % of the cases for N even and 50 % for N odd. The spherical shape gives rise to the occurrence of vibrational structure, and the deformed shape to rotational bands.

The advantage of the mean-field method is that it can be applied directly to the IBM as well. The use of coherent states circumvents the use of coefficients of fractional parentage, and allows one to associate different regions of the parameter space with geometric shapes.

There are many open questions in this area of research. Although the results in the case of the collective boson models can be explained by the allowed shape distributions, there is still no clear explanation for the dominance of $L = 0$ ground states in fermion systems in the context of the shell model. For example, a recent analysis for single j -shell random Hamiltonians displays strong oscillations for the $L = 0$ ground state percentage as a function of j [14], reminiscent of the variations found for the IBM and the vibron model as a function of the boson number N [5]. The role of the approximate conservation of seniority should be further investigated. Another outstanding question is whether an appropriate truncation of the shell model space can lead to vibrational and rotational correlations of the kind observed in the IBM. Can shape be more precisely defined, for example, in a restricted fermion-paired Hilbert space? These and other studies are in progress.

Acknowledgements

We thank S. Pittel and D. Rowe for interesting discussions. This work was supported in part by CONACYT under projects 32416-E and 32397-E, and by DPAGA under project IN106400.

References

- [1] C.W. Johnson, G.F. Bertsch and D.J. Dean, Phys. Rev. Lett. **80** (1998), 2749.
- [2] C.W. Johnson, Rev. Mex. Fís **45 S2** (1999), 25.
- [3] R. Bijker, A. Frank and S. Pittel, Phys. Rev. C **60** (1999), 021302.
- [4] R. Bijker and A. Frank, Phys. Rev. Lett. **84** (2000), 420.
- [5] R. Bijker and A. Frank, Phys. Rev. C **62** (2000), 014303.
- [6] C.W. Johnson, G.F. Bertsch, D.J. Dean and I. Talmi, Phys. Rev. C **61** (2000), 014311.
- [7] R. Bijker, A. Frank and S. Pittel, Rev. Mex. Fís. **46 S1** (2000), 47.

- [8] See *e.g.* the reviews T.A. Brody, J. Flores, J.B. French, P.A. Mello, A. Pandey and S.S.M. Wong, *Rev. Mod. Phys.* **53** (1981), 385, and T. Guhr, A. Müller-Groeling, H.A. Weidenmüller, *Phys. Rep.* **299** (1998), 189.
- [9] J.B. French and S.S.M. Wong, *Phys. Lett. B* **33** (1970), 449; *Phys. Lett. B* **35** (1971), 5.
- [10] O. Bohigas and J. Flores, *Phys. Lett. B* **34** (1971), 261; *Phys. Lett. B* **35** (1971), 383.
- [11] R.F. Casten, N.V. Zamfir and D.S. Brenner, *Phys. Rev. Lett.* **71** (1993), 227.
- [12] N.V. Zamfir, R.F. Casten and D.S. Brenner, *Phys. Rev. Lett.* **72** (1994), 3480.
- [13] D. Mulhall, A. Volya and V. Zelevinsky, *Phys. Rev. Lett.* **85** (2000), 4016.
- [14] Y.M. Zhao and A. Arima, RIKEN preprint, August 2000.
- [15] D. Kusnezov, N.V. Zamfir and R.F. Casten, *Phys. Rev. Lett.* **85** (2000), 1396.
- [16] D. Kusnezov, *Phys. Rev. Lett.* **85** (2000), 3773.
- [17] R. Bijker and A. Frank, *Phys. Rev. Lett.*, in press.
- [18] F. Iachello and A. Arima, *The interacting boson model* (Cambridge University Press, 1987).
- [19] A. Frank and P. van Isacker, *Algebraic methods in molecular and nuclear structure physics*, (Wiley, New York, 1994).
- [20] F. Iachello and R.D. Levine, *Algebraic theory of molecules*, (Oxford University Press, Oxford, 1995).
- [21] F. Iachello, *Chem. Phys. Lett.* **78** (1981), 581.
- [22] F. Iachello, *Phys. Rev. C* **23**, (1981), 2778.
- [23] F. Iachello, N.C. Mukhopadhyay and L. Zhang, *Phys. Rev. D* **44** (1991), 898.
- [24] O.S. van Roosmalen and A.E.L. Dieperink, *Ann. Phys. (N.Y.)* **139** (1982), 198; S. Levit and U. Smilansky, *Nucl. Phys. A* **389** (1982), 56.

Table 1: Probabilities and percentages for ground states with angular momentum L in the decoupling limit

Ground State	N even		N odd	
	Prob.	Perc.	Prob.	Perc.
$L = 0$	$\frac{1}{2}(1 + P_1)$	69.8 %	$P_1 + \frac{1}{2}P_2$	50.4 %
$L = 1$	--	0.0 %	$\frac{1}{2}(1 - P_1 - P_2)$	19.4 %
$L = N$	$\frac{1}{2}(1 - P_1)$	30.2 %	$\frac{1}{2}(1 - P_1)$	30.2 %

Table 2: Percentages of $L = 0$ ground states, calculated in the decoupling limit (mf) and with the moment of inertia (\mathcal{I}). The exact results are based on 100,000 runs with $N = 20$ and $N = 21$.

Shape	N even		N odd		R
	mf	\mathcal{I}	mf	\mathcal{I}	
$\alpha_0 = 0$	39.6 %	39.5 %	39.6 %	39.5 %	2
$0 < \alpha_0 < 1$	10.8 %	13.8 %	10.8 %	13.8 %	3
$\alpha_0 = 1$	19.4 %	17.9 %	0.0 %	0.0 %	0
Total	69.8 %	71.2 %	50.4 %	53.3 %	
Exact		71.2 %		54.7 %	

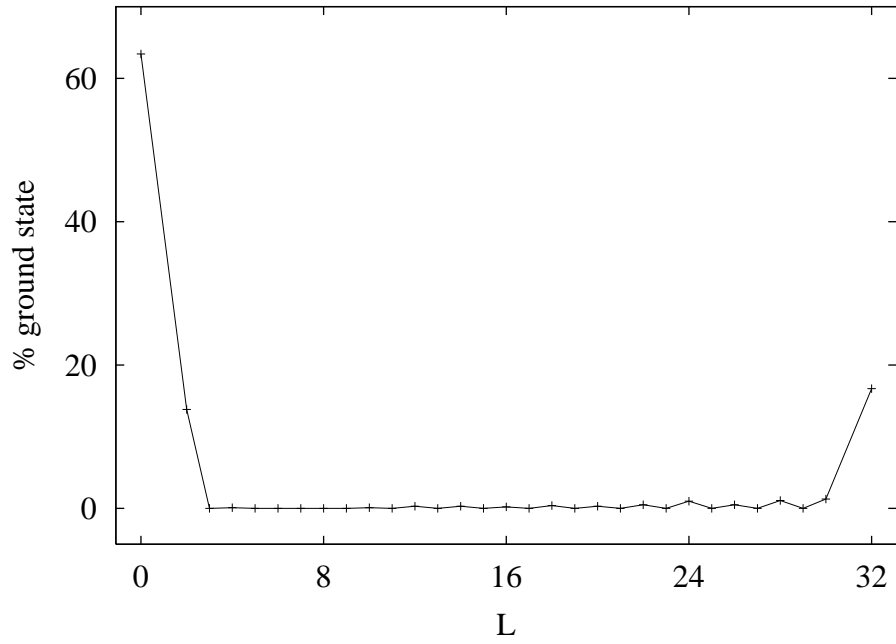


Figure 1: Percentage of ground states with angular momentum L in the IBM with random one- and two-body interactions obtained for $N = 16$ and 1,000 runs.

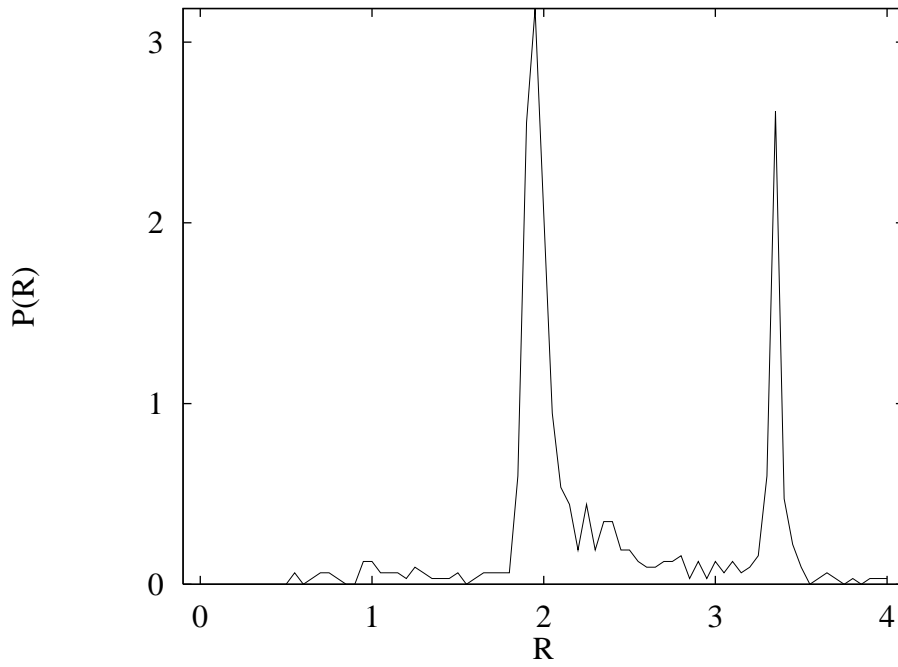


Figure 2: Probability distribution $P(R)$ of the energy ratio R of Eq. (1) in the IBM with random one- and two-body interactions obtained for $N = 16$ and 1,000 runs.

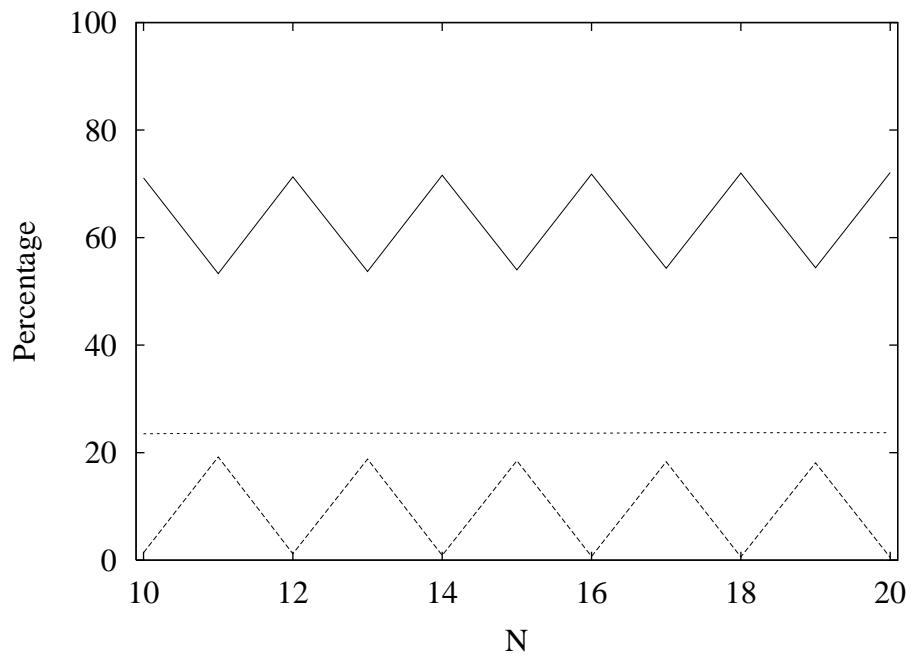


Figure 3: Percentage of ground states with angular momentum $L = 0$ (solid line), $L = 1$ (dashed line) and $L = N$ (dotted line) in the vibron model with random one- and two-body interactions obtained for $10 \leq N \leq 20$ and 100,000 runs.

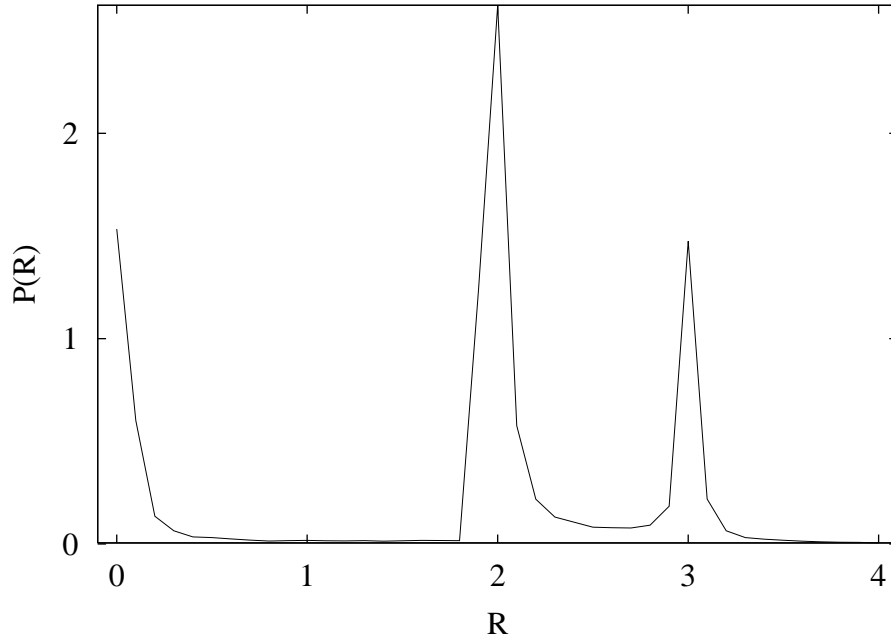


Figure 4: Probability distribution $P(R)$ of the energy ratio R of Eq. (7) in the vibron model with random one- and two-body interactions obtained for $N = 20$ and 100,000 runs.

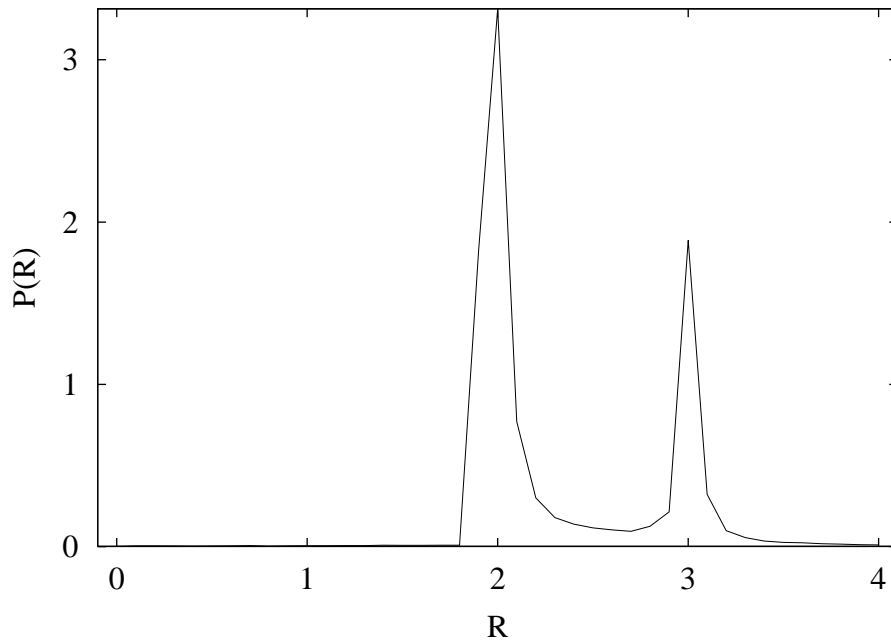


Figure 5: As Fig. 4, but for $N = 21$.

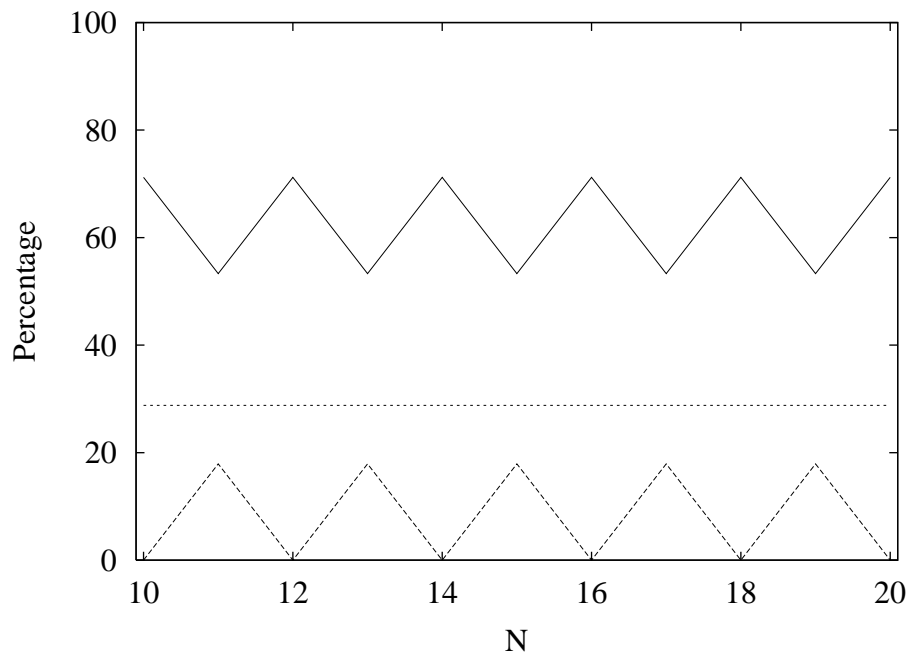


Figure 6: Percentage of ground states with angular momentum $L = 0$ (solid line), $L = 1$ (dashed line) and $L = N$ (dotted line) in the vibron model with random one- and two-body interactions obtained in a mean-field analysis for $10 \leq N \leq 20$.